

Comparison of bar strengths in active and non-active galaxies

Eija Laurikainen,[★] Heikki Salo and Pertti Rautiainen

Division of Astronomy, Department of Physical Sciences, FIN-90014, Finland

Accepted 2001 December 6. Received 2001 December 6; in original form 2001 September 14

ABSTRACT

From an original sample of 107 spiral galaxies, the bar strengths of 21 active galaxies are compared with those of 22 non-active galaxies. Our identifications of bars are inferred from near-IR images using Fourier methods. The bar torques are determined using a new technique due to Buta & Block, in which tangential forces are calculated in the bar region normalized to the axisymmetric radial force field. As a data base we use the *JHK* images of the 2 Micron All Sky Survey. The ellipticities ϵ of the bars are also estimated with an isophotal fitting algorithm and the bar lengths from the phases of $m = 2$ and $m = 4$ Fourier components of density. We show a first clear indication that the ellipticity of a bar, generally used as a measure of the bar strength, is quite well correlated with the maximum relative tangential force, Q_b , in the bar region.

Most surprisingly, the galaxies with the strongest bars are non-active. A possible understanding of this unusual result is that previous gaseous inflow in such cases may have been so efficient that fuelling of the active nuclei may simply have ceased. We find that nuclear activity occurs preferentially in those barred early-type galaxies in which the maximal bar torques are weak ($\langle Q_b \rangle = 0.21$) and appear at quite large distances from the galactic centre when scaled with the radial scalelength of the disc ($\langle r_{Q_b}/h \rangle = 1.24$). For comparison, for the non-active galaxies $\langle Q_b \rangle = 0.37$ and $\langle r_{Q_b}/h \rangle = 0.59$. The force maximum in the active late-type galaxies also appears at rather large distances, but the difference from the non-active galaxies is smaller. These results imply that the bulges may be important for the onset of nuclear activity, but it is not clear why nuclear activity appears in some early-type galaxies but is missing from some others. We also find that for active early-type galaxies, bar length is not correlated with bar strength, although a weak correlation appears for the other barred galaxies studied.

Key words: gravitation – instabilities – methods: statistical – galaxies: active – galaxies: nuclei – galaxies: Seyfert.

1 INTRODUCTION

It is now widely accepted that non-axisymmetric forces are needed to trigger nuclear activity by accreting gas to the central regions of galaxies. Primary bars are known to be efficient for dragging gas on scales larger than 1 kpc, but some other mechanism is needed to allow this gas finally to fall into the active nucleus, provided for example by secondary bars (Shlosman, Frank & Begelman 1989). Indeed, star formation is found to be enhanced in barred galaxies (Martinet & Friedli 1997; Aquerri 1999), but the connection between bars and nuclear activity (AGNs in terms of accretion discs and black holes) is not clear observationally. For example, there is no indisputable agreement showing that the number of bars is larger for AGNs in comparison with non-active systems. An

excess of bars in AGNs is found by some authors (Knapen, Shlosman & Peletier 2000; Laine et al. 2001), while most studies give similar bar fractions for active and non-active galaxies (McLeod & Rieke 1995; Moles et al. 1995; Ho, Filippenko & Sargent 1997; Mulchaey & Regan 1997; Hunt & Malkan 1999; Marquez et al. 2000). Bars can act as driving forces for the central activity via the strong inflow of gas in shock regions associated with the rotating bar potential. Not surprisingly, the nuclear regions of barred galaxies have on average higher concentrations of molecular gas than normal galaxies (Sakamoto, Baker & Scoville 2000; Sheth 2001), which makes understandable the connection found between bars and high star-formation activity.

Star-formation activity is found to be correlated with the properties of bars, being enhanced especially in long bars with high ellipticities, usually regarded as ‘strong’ bars (Martinet & Friedli 1997; Aquerri 1999). However, not all long bars have pronounced

[★]E-mail: eija.laurikainen@oulu.fi

current star-formation activity. On the other hand, it has been suggested that Seyferts may even avoid ‘strong’ bars (Shlosman, Peletier & Knapen 2000; Laine et al. 2001), but this has been questioned by Marquez et al. (2000), who argued that both the lengths and strengths of the primary bars are similar for Seyferts and for non-Seyfert galaxies. In all these works bar strength is estimated indirectly from the ellipticity of a bar, based on analytical work by Athanassoula (1992a).

The size of a bar is related to the Hubble type so that bars in early-type systems are generally longer than in late-type systems, when normalized to the galaxy diameter at 25 magnitude isophote D_{25} (Elmegreen & Elmegreen 1985; Duval & Monnet 1985; Martin 1995; Regan & Elmegreen 1997). Also, Elmegreen & Elmegreen (1985) find a weak correlation between the bar axial ratio and the Hubble type, but this has not been confirmed by Martin (1995) using a larger sample of galaxies. Elmegreen & Elmegreen (1985) also showed that bars in early-type galaxies are generally flat, while those in late-type systems are exponential. Altogether, the Hubble type is expected to be an important factor in controlling the properties of bars and probably also the inflow of gas.

The ellipticity of a bar is not a full description of its strength, depending also on the mass of the bar. Moreover, the relative perturbation associated with the bar depends on the central force field, i.e. the presence of a massive bulge. Therefore bar strengths are better evaluated by the tangential forces normalized to the total axisymmetric force fields, as suggested by Combes & Sanders (1981) and applied for galaxies by Buta & Block (2001). We use a similar approach and determine bar torques for 107 spiral galaxies in *JHK*-bands. Fourier analysis is used to identify bars, and for those galaxies with well-defined bars, strengths are compared between the active and non-active galaxies. We also test how well the bar strength and the ellipticity of a bar are correlated.

2 THE SAMPLE AND THE METHOD

The original sample consists of those spiral galaxies with $B_T < 12.5$ mag, $cz < 2500$ km sec⁻¹ and $i < 67^\circ$ in the Third Reference Catalog of Bright Galaxies (de Vaucouleurs et al. 1991, hereafter RC3), for which high-quality images were available in the 2 Micron All Sky Survey (hereafter 2MASS). By ‘*i*’ we denote the inclination of the galactic disc. Additionally, some of the weakest objects were eliminated so that the number of galaxies in the sample was 107. In the active galaxy category we include Seyferts, LINERs and H II galaxies, for which the spectral classifications were taken from the NASA/IPAC Extragalactic Database (NED), where the latest spectral classifications are available. Altogether, 53 of the galaxies show nuclear activity and 31 are classified as barred (SB) in RC3. The image resolution is one arcsecond per pixel and the H-images are generally deeper than the images in the *J*- or *K*-bands. The selection effects of the sample are discussed by Laurikainen & Salo (2002). We found that the frequency of bar identifications rapidly decreased when the inclination of the disc is larger than 50° . Also, the non-active galaxies appeared to be on the average somewhat brighter than the active galaxies. Considering that the absolute brightnesses of the galaxies correlate with the bar lengths, somewhat longer bars are thus selected for the active galaxies. However, we also estimated that these biases do not affect our conclusions.

The distribution of optical morphological types for active galaxies in our sample is quite similar to that found previously for Seyferts in larger samples of galaxies, the active galaxies being

shifted toward earlier Hubble types. The peak appears for Sab types, which is between the mean morphological types for Seyfert 1 (Sa) and Seyfert 2 (Sb) galaxies by Malkan, Gorjian & Tam (1998). If we exclude H II galaxies, the active systems are even more clearly concentrated towards early Hubble types. In the following, the galaxies will be divided to early (SO/a, Sa, Sab), late (Sbc, Sc, Scd) and very-late types (later than Scd), based on the classification in RC3. The omission of the seven latest-type systems from the category of late-type galaxies is justified by the fact that for types later than Scd the bulge-to-disc ratio does not follow the general decreasing tendency from early to later types in the Hubble sequence (de Jong 1996), a phenomenon that has been discussed theoretically by Noguchi (2000).

A large majority of spiral galaxies are now considered to have bar-like potentials, wherein bars lie on a continuous scale from zero to six bar torque classes (Buta & Block 2001). Our identification of bars does not rely on optical morphological classifications. Rather, the presence of a bar was confirmed if the phases of the $m = 2$ and $m = 4$ Fourier components of density were maintained nearly constant in the bar region. Additionally, it is required that the maximum $m = 2$ component has a high amplitude. In this paper we exclude those bars/ovals whose $m = 2$ amplitude, normalized to the $m = 0$ component, lies below 0.3. The length of the region where the phase is maintained nearly constant also determines the length of the bar. We thus find 43 barred galaxies in the near-IR, clearly exceeding the number of barred galaxies in the optical – in agreement with earlier studies based on near-IR images (Block & Wainscoat 1991; Knapen et al. 2000; Eskridge & Frogel 1999). Also, all galaxies classified as SB in RC3 appeared to be barred in the near-IR. In principle, our method of calculating bar strengths does not require any pre-identification of a bar, but here we wanted to concentrate only on galaxies that were clearly barred.

Bar strengths were determined by transforming the light distributions into potentials and deriving the maximum ratios of the tangential forces relative to the radial forces. This approach was first suggested by Combes & Sanders (1981), but has been systematically applied for galaxies only recently by Buta & Block (2001), who used the potential evaluation method due to Quillen, Frogel & Gonzalez (1994) for the force calculation. In order to obtain a single measure for the strength we use Q_b , which is the maximum of Q_T in the bar region (as in Buta & Block 2001). The distance where the maximum of Q_T occurs is denoted by r_{Q_b} . For the galaxy distances we used the measurements by Tully (1988).

Our method of force calculation is not completely identical with that of Buta & Block, its full description being presented by Laurikainen & Salo (2002). For example, owing to the limited resolution of the 2MASS images the gravitational potential was not calculated with cartesian integration from the original images. Instead, the images were first ‘smoothed’ by calculating the azimuthal Fourier decompositions of the surface densities in different radial zones, in a way similar to that done by Salo et al. (1999). In the calculations, the even Fourier modes from 2 to 10, characteristic of bars (see Ohta 1996), were included. Also, instead of using the vertical scaleheight of the Milky Way as done by Buta & Block, the scaleheight was taken to be a certain fraction of the radial scalelength of the disc.

The mass density in the vertical direction was approximated by an exponential model. Following de Grijs (1998) we used $h/h_z = 2.5$ for the early-type galaxies and $h/h_z = 4.5$ for the late-type systems. The exponential scalelengths were taken from the catalogue of Baggett, Baggett & Anderson (1998) when available,

and otherwise they were estimated from the 2MASS images by us. For a few cases where h was not given by Baggett et al. and could not be determined from the 2MASS images either, the scaleheight of the Milky Way ($h_z = 325$ pc) was used. These galaxies are omitted from those plots, where the bar parameters are scaled to h . For three of the galaxies, pgc 10266, pgc 15821 and pgc 40097, the scalelength given by Baggett et al. was considered to be unrealistic. For two of them h was rather a measure for the brightness slope in the bulge region, whereas for pgc 10266 the given scalelength represented the outermost very shallow part of the disc, while we are interested in the disc under the bar. Also for these three galaxies the assigned scalelengths were measured from the 2MASS images.

The ellipticity of a bar, generally used as a measure of the bar strength, is an approximation of the true bar strength. Therefore, for comparison the maximum ellipticities were also determined by fitting ellipses to the isophotes of the surface brightnesses, as described by Laurikainen & Salo (2000). The ellipticity of a bar was taken to be that of the smallest deprojected minor-to-major axis ratio $\epsilon = 1 - (b/a)_{\min}$. Our measurements are in good agreement with those by Laine et al. (2001) for six barred galaxies common in our samples, both regarding ϵ and the semimajor axis of the most elongated isophote (r_ϵ) (see Fig. 1). The mean values of Q_b , ϵ and their radial distances for the different subsamples are shown in Table 1. The errors in the table denote the sample standard deviations. For Q_b the largest source of uncertainty is in fact due to the uncertainty in the vertical scaleheight, which for example for Sc-galaxies varies by $h/h_z = 2.5$ to 5.5 (de Grijs 1998). This corresponds to an uncertainty of about 15 per cent in Q_b . Notice that the uncertainty in h_z does not affect r_{Q_b} .

3 STRENGTHS OF THE NON-AXISYMMETRIC FORCES

In the following, non-axisymmetric forces are compared between the active and non-active barred galaxies. Since the measurements in the J -, H - and K -bands give very similar results, only those related to H -images are reported. Bar strengths between the early- and late-type galaxies are also compared. This is important because the Hubble type to some extent measures the bulge-to-disc ratio (B/D) for a galaxy and the bulge might be an important factor in controlling the properties of bars and nuclear activity. The B/D-ratio varies along the Hubble sequence similarly in the optical and in the near-IR (de Jong 1996).

Before doing any such comparisons between different galaxy subsamples it is interesting to verify how well the maximum isophotal ellipticity ϵ of a bar and the maximal non-axisymmetric force Q_b , are correlated. Indeed, we found rather tight correlation between these two parameters (see Fig. 2). We show here $b/a = 1 - \epsilon$, to make it easier to compare with the similar plot by Block et al. (2001). Fig. 2 also uses different symbols for various subsamples, indicating that there is a small difference between the early- and late-type galaxies in the diagram, being largely due to the larger vertical scaleheight used for the early-type galaxies: if the same h/h_z is used for all galaxies, the difference disappears. This correlation is the first direct observational confirmation showing that the bar axial ratio is indeed a good measure of the bar strength. However, it is worth noticing that especially when the ellipticity of a bar is high, even a small change in the elongation of a bar results in a large change in the non-axisymmetric force. Therefore, Q_b is a more sensitive measure of the bar strength even for strong bars.

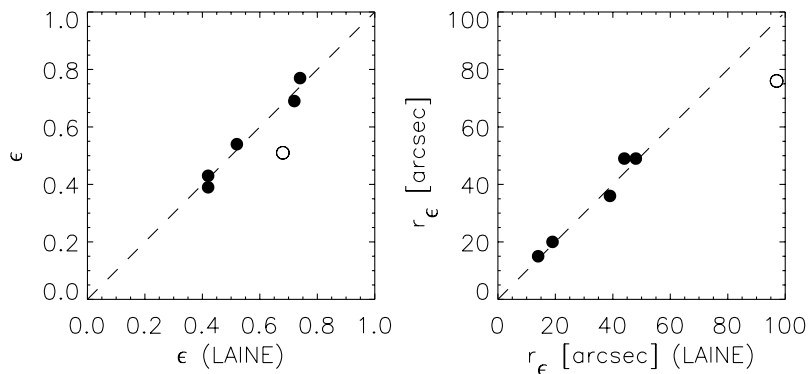


Figure 1. Comparison of the maximum ellipticities of bars ($\epsilon = 1 - b/a_{\min}$) and the locations of the most elongated isophotes (r_ϵ) between the measurements by Laine et al. (2001) and us, for the six galaxies common in our samples. Notice the very good agreement except for one galaxy (open symbol). For that galaxy, the 2MASS-image we use is not deep enough to reveal the region of maximum ellipticity.

Table 1. Mean maximum tangential forces, maximum ellipticities and the locations of the maxima, as well as bar lengths for barred galaxies. The errors denote the sample standard deviations.

	N	$\langle Q_b \rangle$	$\langle r_{Q_b}/h \rangle$	$\langle r_{\text{bar}}/h \rangle$	$\langle \epsilon \rangle$	$\langle r_\epsilon/h \rangle$
Active	21	0.27 ± 0.13	1.15 ± 0.61	1.85 ± 0.79	0.57 ± 0.11	1.40 ± 0.77
Non-active	22	0.37 ± 0.23	0.59 ± 0.30	1.26 ± 0.52	0.60 ± 0.14	0.83 ± 0.44
Early	19	0.25 ± 0.13	1.04 ± 0.61	1.80 ± 0.82	0.56 ± 0.12	1.31 ± 0.72
Late	21	0.38 ± 0.23	0.73 ± 0.46	1.39 ± 0.60	0.61 ± 0.12	1.00 ± 0.62
Active early	14	0.21 ± 0.07	1.24 ± 0.58	1.99 ± 0.83	0.53 ± 0.09	1.50 ± 0.73
Active late	6	0.40 ± 0.13	0.92 ± 0.73	1.58 ± 0.76	0.67 ± 0.06	1.11 ± 0.90
Non-active early	5	0.35 ± 0.19	0.51 ± 0.28	1.27 ± 0.54	0.63 ± 0.17	0.77 ± 0.33
Non-active late	17	0.38 ± 0.25	0.61 ± 0.32	1.25 ± 0.53	0.60 ± 0.13	0.85 ± 0.49

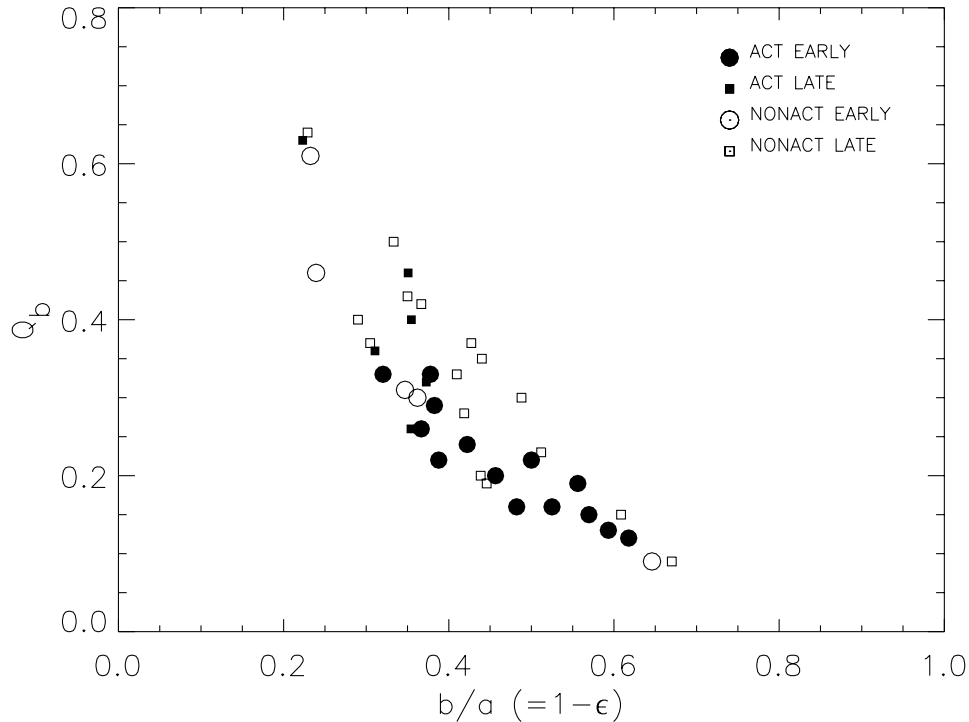


Figure 2. Bar strength Q_b versus minor-to-major axis ratio for the galaxies in our sample. The active and non-active early- and late-type galaxies are shown separately with different symbols (same in all the subsequent figures). In order to have our figure to be easily comparable with that by Block et al. (2001), b/a was used instead of ϵ .

A correlation between Q_b and b/a was found also by Block et al. (2001), but the dispersion was two or three times larger than in our similar diagram. Based on this scatter, they suggested that apparently bars with significant ellipticities may be either strong, weak or intermediate as far as the relative bar torques are concerned. However, on the basis of our result this probably is not the case. We rather suppose that the most important reason for the large scatter was the high uncertainty in the b/a values by Martin (1995) that Block et al. used. Martin estimated the uncertainties of ϵ to be about 20 per cent. The uncertainties are large, because the lengths of the major and minor axes were estimated visually without any isophotal-fitting routine. Also, blue photographic plates were used which might be another cause for the large scatter: the near-infrared images that we use are better expected to trace the true mass distribution in the bar region than the blue images. The fact that Block et al. included also the SAB-galaxies in their diagram hardly explains their scatter, because it was also large in the region with $Q_b > 0.3$, where only SB-galaxies appeared.

When all barred galaxies are considered (see Fig. 3, Table 1) it seems that active galaxies might have on the average smaller non-axisymmetric forces than the non-active systems ($\langle Q_b \rangle = 0.27$ versus 0.37). However, while applying the Kolmogorov–Smirnov test (KS-test) this difference is only marginally significant: the probability that the samples are drawn from similar populations is $p = 0.10$. A similar result, but with no statistical significance ($p = 0.37$) was obtained for the ellipticities of bars. Our result for the ellipticities is in accordance with Shlosman et al. (2000) and Laine et al. (2001). In our preliminary study (Laurikainen, Salo & Rautiainen 2001), it was argued that the difference in Q_b between the active and non-active galaxies is statistically significant with $p = 0.05$. The reason for the slightly lower statistical confidence level in the current study is that here the sample has been somewhat reduced by lowering the upper inclination limit. Also, bar strengths

for a few galaxies have been re-measured using more appropriate scalelengths for the discs.

However, statistically significant differences appear between the active and non-active galaxies for the locations of the maximum tangential forces, r_{Q_b}/h , and in the radial distances of the maximum ellipticities, r_ϵ/h . These maxima appear at much larger distances from the galactic centre for the active than for the non-active galaxies (Fig. 3, Table 1). The probabilities that the compared samples are drawn from similar populations are $p = 0.0008$ and 0.007 for r_{Q_b}/h and r_ϵ/h , respectively. As the r_{Q_b}/h – value is quite sensitive to the scalelength of the disc, we normalized r_{Q_b} also to the diameter at the contour level of 25 mag arcsec $^{-1}$ D_{25} , but this did not affect the conclusions or the level of the statistical significances in the comparisons. The difference in the barred properties between the active and non-active galaxies is even more illustrative while correlating Q_b with r_{Q_b}/h , as shown in Fig. 4. It is remarkable that almost all galaxies with $r_{Q_b}/h > 1$ are active, while for the non-active galaxies r_{Q_b}/h is rather small even for the strongest bars. An important point to stress here is that due to their morphological distributions the active galaxies largely follow the distribution of early-type galaxies, whereas the non-active galaxies behave much like the late-type systems. Thus the difference we find might simply indicate a difference between the early- and late-type spirals. However, the connection between the activity and the Hubble type is not that straightforward, as will be discussed in the following.

The radial Q_T -profiles for the individual barred galaxies are presented in Fig. 5, showing separately the active and the non-active early- and late-type galaxies. While comparing the average bar strengths we can see that in fact only the early-type active galaxies have noticeably smaller bar strengths, with the mean $\langle Q_b \rangle = 0.21$. All the other subsamples, such as the non-active early-type galaxies and the late-type systems have larger $\langle Q_b \rangle$

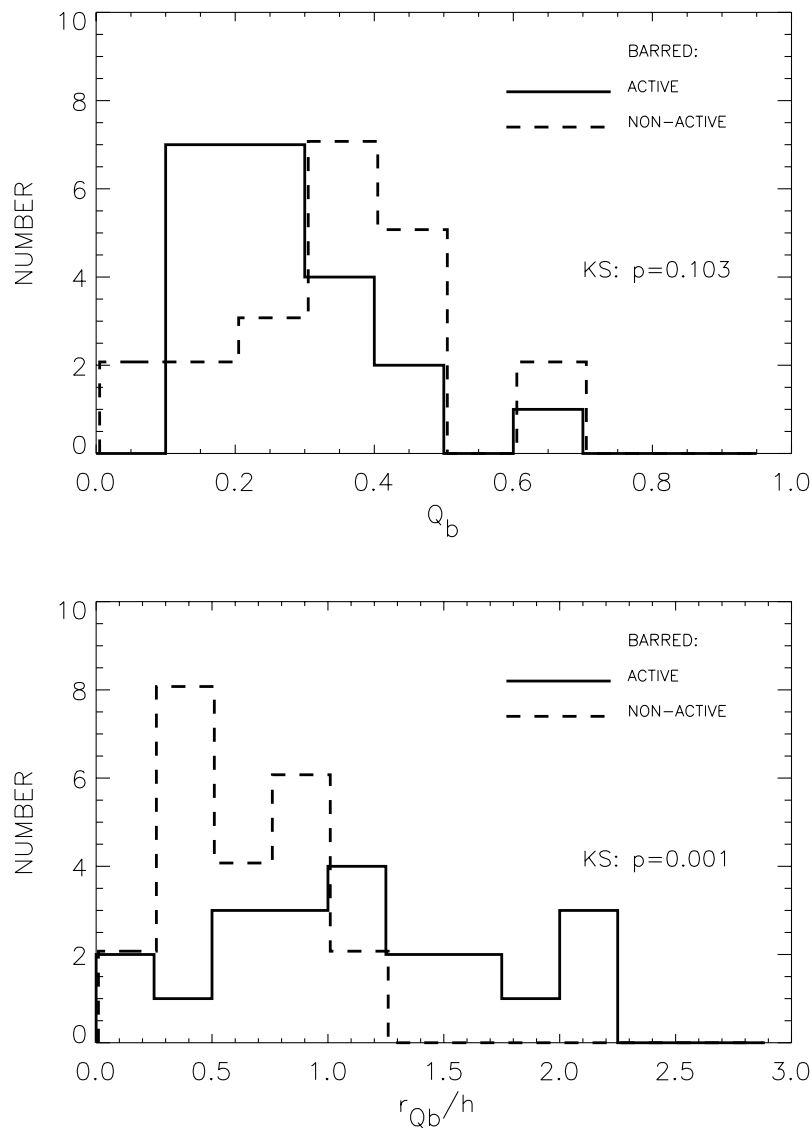


Figure 3. The histograms of the maximum tangential forces Q_b and their distances r_{Q_b}/h for the barred active and non-active galaxies are compared. The distances are scaled to the scalelength of the disc, largely taken from Baggett et al. (1998) or measured from the 2MASS images by us. In the Q_b -histogram one non-active galaxy has $Q_b = 1.4$, which was left out of the histogram.

values between 0.35 and 0.40 (see Table 1). The KS-test shows that the probability that the samples of active and non-active early-type galaxies are drawn from similar populations is $p = 0.04$ and $p = 0.02$ for Q_b and ϵ , respectively, which means that these differences are statistically significant.

It is also clear that the distances of the ellipticity maxima and the maximal tangential forces are largest for the active early-type galaxies with $\langle r_{Q_b}/h \rangle = 1.24$ and $\langle r_\epsilon/h \rangle = 1.50$, respectively (see Fig. 5 and Table 1). For the active late-type systems these parameters show somewhat lower values with $\langle r_{Q_b}/h \rangle = 0.92$ and $\langle r_\epsilon/h \rangle = 1.11$, but they are still higher than for the non-active galaxies with $\langle r_{Q_b}/h \rangle = 0.51$ – 0.61 and $\langle r_\epsilon/h \rangle = 0.77$ – 0.85 . These results show that the bulges alone cannot explain why especially the active early-type galaxies have small Q_b and large r_{Q_b} -values.

4 BAR LENGTHS

The lengths of the bars were estimated both by Fourier techniques (r_{bar}) and by the maximal ellipticities of bars (r_ϵ). In Laurikainen &

Saló (2002) the absolute bar length in kiloparsecs was found to correlate with the absolute brightness of the galaxy, in agreement with Kormendy (1979), but while scaling the bar length to the scalelength of the disc, the correlation disappeared. Therefore, when using the scaled bar lengths (r_{bar}/h), there is no need to worry about possible magnitude biases in the compared samples. We found that r_{bar} correlates with r_ϵ for all Hubble types and activity classes (see Fig. 6, lower panel). However, r_ϵ gives systematically shorter bar lengths, which means that r_ϵ is not a very reliable measure of the bar length, often underestimating the true bar length. In fact, in many N -body simulations the bar ellipticity can decrease considerably before the actual end of the bar (Rautiainen & Saló 1999). The distance r_ϵ is also correlated with r_{Q_b} , but in such a way that the force maximum appears systematically at shorter distances than the ellipticity maximum (see Fig. 6, upper panel).

We confirm the earlier result by Elmegreen & Elmegreen (1985), Martin (1995) and Regan & Elmegreen (1997) showing that early-type galaxies have on the average longer bars than late-type

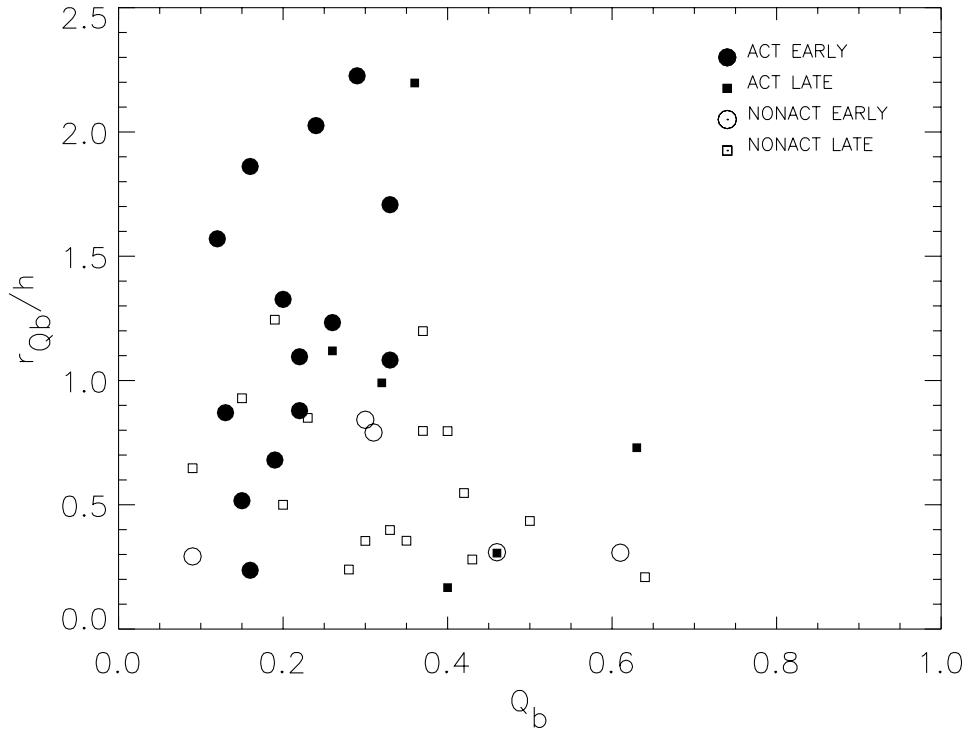


Figure 4. The distance of the maximum non-axisymmetric force r_{Q_b}/h versus the maximum force Q_b , shown separately for the active and the non-active early- and late-type barred galaxies in our sample.

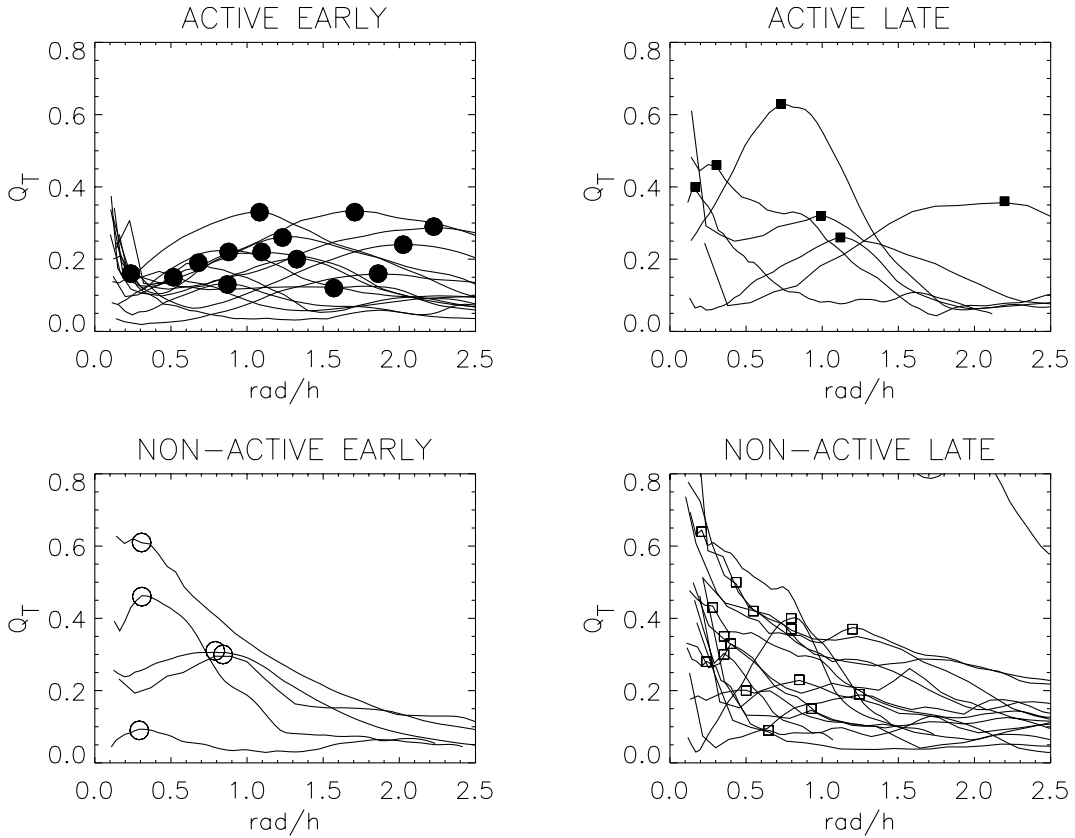


Figure 5. The radial Q_T -profiles for the active and the non-active early- and late-type barred galaxies. The radii are scaled to the scalelength of the disc. The symbols denote the location of the assigned maximum Q_T -values. Note that for some late-type systems the Q_T -profiles rise monotonically toward the centre: in these cases the maximum was estimated by eye, eliminating the possible contribution of the artificial bulge elongation in the de-projection. The uncertainty of these cases does not affect our conclusions.

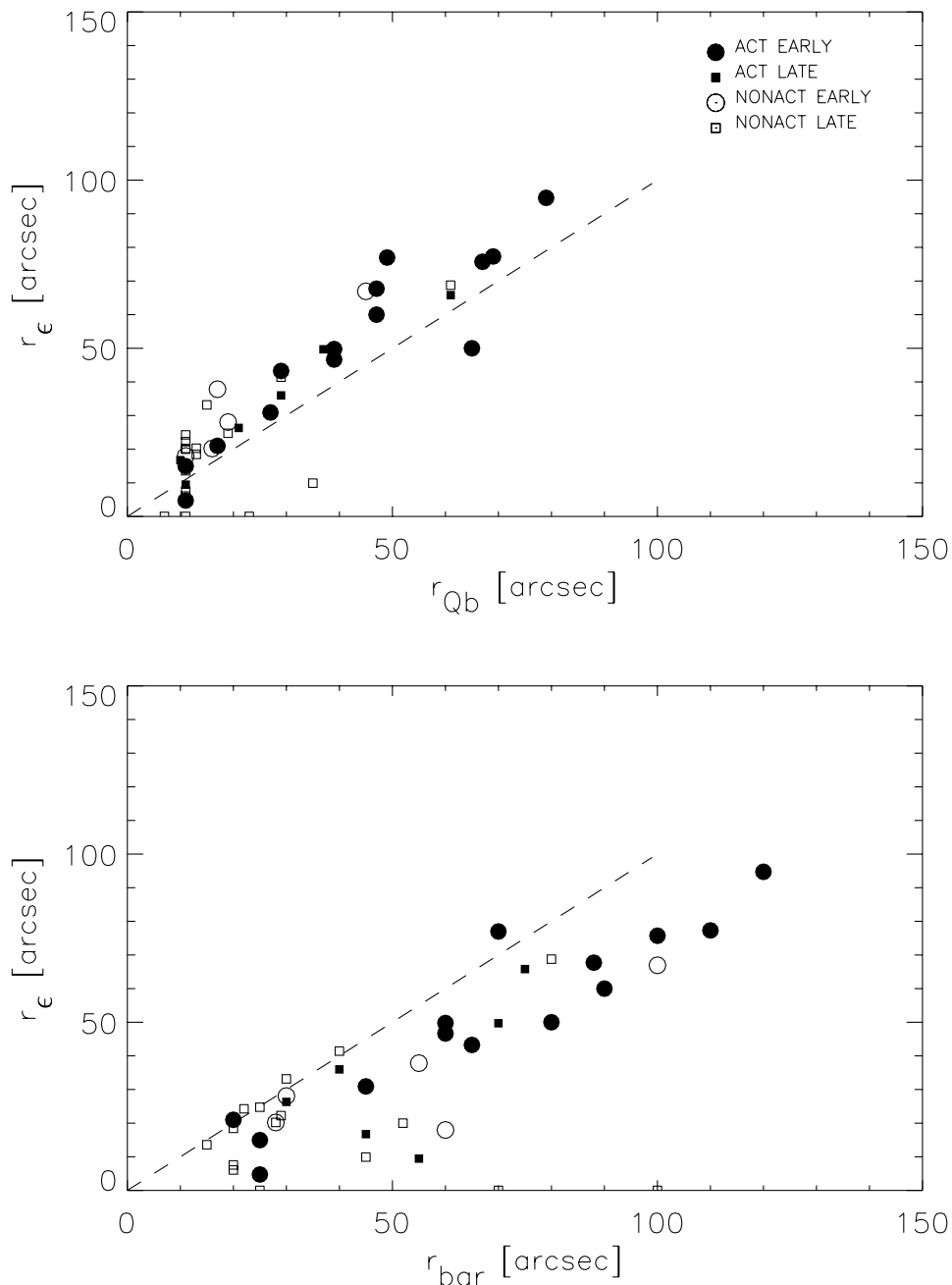


Figure 6. In the upper frame the relation between the distances of the force maxima r_{Q_b}/h and the ellipticity maxima r_ϵ/h is shown, while in the lower frame r_ϵ is plotted against r_{bar} . Notice that in the upper frame the symbols at $r_{Q_b} = 10$ correspond to our adopted lower limit of r_{Q_b} . Likewise for the cases with $r_\epsilon = 0$ no definite value for r_ϵ could be obtained.

systems (see Table 1), but the difference we find is smaller than suggested by Martin. In fact, the samples by Martin and Regan & Elmegreen are not very representative for early-type spirals: Regan & Elmegreen have only 1 early-type galaxy among 23 galaxies, and Martin has 5 galaxies among 136, classified as SO/a, Sa or Sab. On the other hand, our result is in accordance with the study by Elmegreen & Elmegreen (1985), based on a sample of 99 galaxies, which covers well the whole range of the Hubble sequence for spiral galaxies. As in our work, they also find larger dispersion in bar lengths for the early than for the late-type galaxies, and especially some SO/a galaxies in their sample have very short bars.

When the whole sample of barred galaxies is studied, bar strength Q_b (or ϵ) definitely does not correlate with bar length r_{bar} ,

which is shown in Fig. 7. This is the case both when the bar length is given in kiloparsecs, or scaled to the scalelength of the disc. Therefore, bar length cannot be considered as a measure of bar strength: short bars can have either strong or weak tangential forces. However, if only the late-type or the non-active early-type galaxies are considered, r_{bar} seems to increase slightly with increasing Q_b , which is in accordance with Martin (1995), whose sample consisted mainly of late-type spirals. The surprising thing here is that the active early-type galaxies have rather long bars, even though their strengths are only weak or moderate.

Like bar strengths, also bar lengths for the active and non-active galaxies in our samples are associated with the Hubble type: while bars of active galaxies have lengths rather similar to those of the

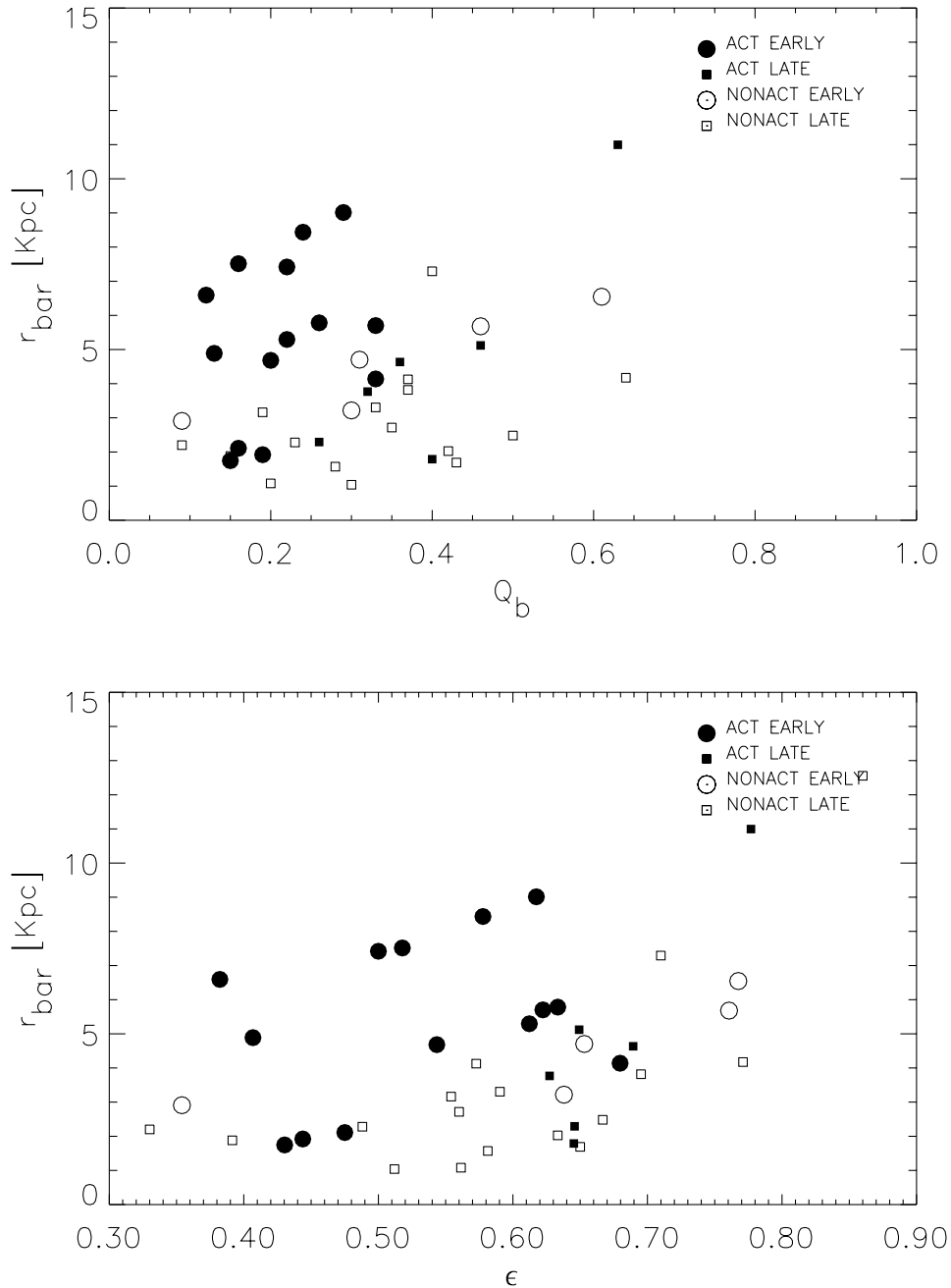


Figure 7. In the upper frame, bar length r_{bar} is plotted as a function of bar strength Q_b for the barred galaxies, and below a similar plot for the ellipticity measurements is shown.

early-type galaxies, bars in non-active systems largely follow the length distribution of late-type galaxies (see Fig. 7). The longest (and at the same time weakest) bars belong to the active early-type galaxies, whereas bars in the late-type galaxies are shorter (see also Table 1). This is a result that should be understood also theoretically: why is it that in bulge-dominated galaxies, where the bulge probably stabilizes the bar region, thus reducing the bar strength, bars are at the same time very long? This will be discussed in Chapter 7.

5 BAR ELLIPTICITY AND TANGENTIAL FORCES: ANALYTICAL TOY MODELS

In order to gain understanding of the dependence found between

Q_b and ϵ , some simple analytical force models were constructed. We use a model potential which consists of a spherical Plummer bulge, an axially symmetric exponential disc and a non-axisymmetric bar, represented by a prolate Ferrers ellipsoid. The bulge and disc are characterized by their masses, M_{bulge} and M_{disc} , and by the bulge radius R_{bulge} and the disc exponential scale-length h . In all cases the ratio $R_{\text{bulge}}/h = 1/5$. The Ferrers ellipsoid has a density function

$$\rho = \begin{cases} \rho_0(1 - g^2)^n & \text{if } g < 1, \\ 0 & \text{if } g > 1, \end{cases}$$

with $g^2 = x^2/a^2 + (y^2 + z^2)/b^2$, where a and b stand for the bar major and minor axis and ρ_0 for its central density, connected to the

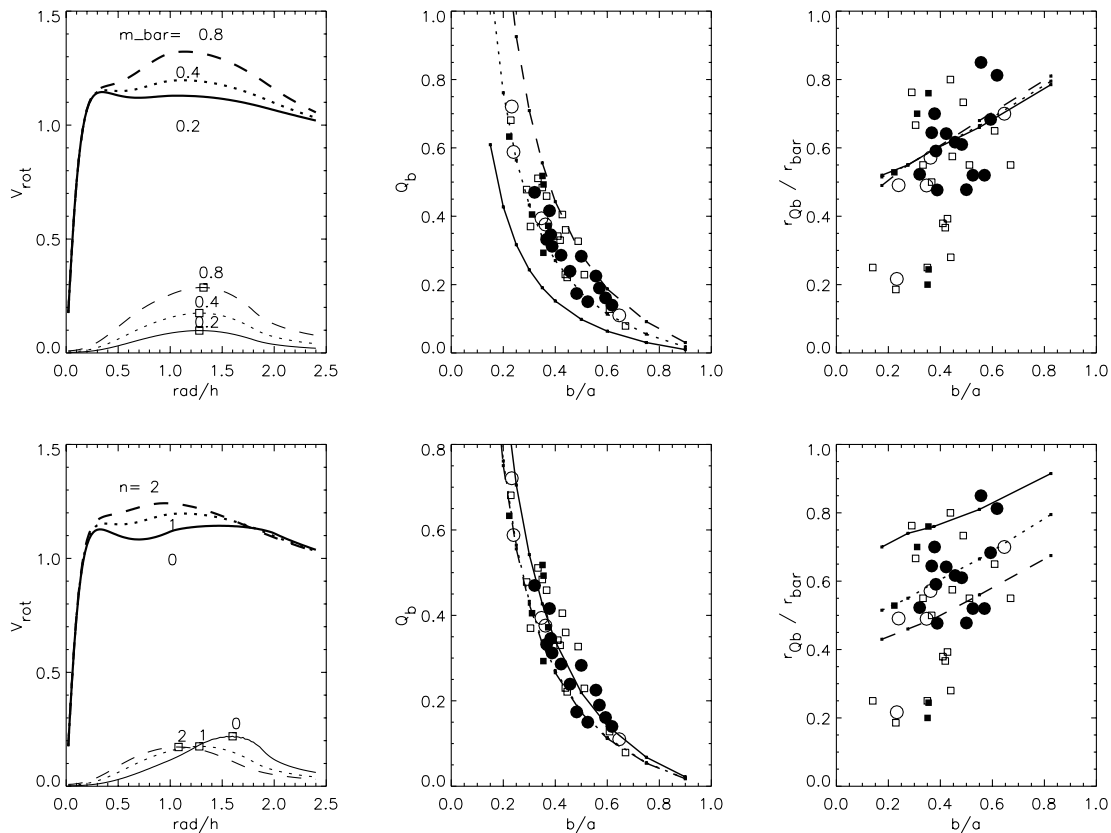


Figure 8. Analytical toy models for the maximum ratio of tangential force to radial force (Q_b) and its location (r_{Q_b}/r_{bar}), for different bar axial ratios (b/a). As explained in more detail in the text, the models consist of a bulge + disc combined with a Ferrers-bar. Here $M_{\text{bulge}}/(M_{\text{bar}} + M_{\text{disc}}) = 0.3$, implying a short rising part of the mean rotation curve. In the upper row $M_{\text{bar}}/(M_{\text{bar}} + M_{\text{disc}}) = 0.2, 0.4, 0.8$ are compared, while a fixed $n = 1$ is assumed. In the lower row $n = 0, 1, 2$ while $M_{\text{bar}}/(M_{\text{bar}} + M_{\text{disc}}) = 0.4$ is fixed. The frames in the left column show the rotation curves (thick curves) as well as the radial Q_T -profiles for $b/a = 0.5$ (thin lines). The middle column displays the corresponding Q_b values, while in the right r_{Q_b}/r_{bar} are shown. Symbols denote our measurements.

total bar mass by $M_{\text{bar}} = 2^{2n+3}\Gamma(n+1)\Gamma(n+2)\Gamma(2n+4)\rho_0\pi ab^2$ (Athanasoula 1983). The values $n = 0, 1, 2$ were considered, $n = 0$ representing a bar with constant density, while in the case $n > 0$ the bar is more centrally condensed. The potential corresponding to the bar density distribution was constructed with the formulae given by Pfenniger (1984), and the radial and tangential force components in the equatorial plane $z = 0$ were obtained by numerical differentiation. As advised by Pfenniger (1984), the forces were checked by observing that the Poisson equation was satisfied. The mean radial force due to bar was obtained from the average over different azimuthal directions. In all models, the length of the bar major axis was fixed at $a = 2h$.

In the construction of Q_T -profiles, two basic rotation curve models were studied, differing in the amount of bulge mass with respect to the combined bar + disc mass, having $M_{\text{bulge}}/(M_{\text{bar}} + M_{\text{disc}}) = 0.3$ and 0. The combined bar + disc mean radial force was fixed to that due to a bar with $b/a = 0.5$. Thus in the case of different b/a ratio the axisymmetric disc and bulge actually deviate from those defined above, in a manner that would yield the desired total bulge + disc + bar radial force. For very elongated bars the implied radial force due to the bar alone would in some cases exceed the total radial force: these unrealistic models were excluded.

In Figs 8 and 9, the implied Q_b and r_{Q_b}/a distances are studied as a function of b/a ratio, for different values of $M_{\text{bar}}/(M_{\text{bar}} + M_{\text{disc}})$ and n . Also shown are the rotation curves corresponding to the mean radial forces, with slight differences caused by different

$M_{\text{bar}}/(M_{\text{bar}} + M_{\text{disc}})$ and n , as well as examples of Q_T -profiles (for $b/a = 0.5$). The former figure corresponds to the model including the bulge component, being characterized by a steeply rising inner rotation curve, while in the latter figure the bulge is omitted, leading to a more shallow rise of the rotation curve. With our adopted model parameters the rising portions have lengths of about $0.1a$ and $0.5a$. Very roughly, these two models could be interpreted as representing those of early-type spirals (dominant bulge) and late-type spirals (weak bulge). Also shown in the plots are the measured values of Q_b and r_{Q_b}/r_{bar} for the barred galaxies in our sample.

In spite of its simplicity, the Ferrers-bar model seems to account fairly well for the general trend of Q_b versus b/a , suggesting the possibility that the observed scatter arises due to the different bar mass fractions (Fig. 8, upper row). Interestingly, the value of adopted n changes Q_b only very little, suggesting also that more realistic bar profiles might lead to very similar Q_b for a given bar mass (Fig. 8, lower row). On the other hand, the location where maximum tangential force is obtained depends sensitively on n , more concentrated bar models (larger n) leading to smaller r_{Q_b}/a . In the case with no bulge (Fig. 9) the Q_b 's are naturally somewhat increased for a given $M_{\text{bar}}/(M_{\text{bar}} + M_{\text{disc}})$, due to weaker total radial force. The increased length of the rising portion of the rotation curve (\equiv portion of much-reduced mean radial force) is also visible in r_{Q_b}/a , where models with very elongated bars tend to have maxima shifted to very small distances. Altogether, the scatter in observed r_{Q_b}/r_{bar} versus b/a is also rather nicely accounted for.

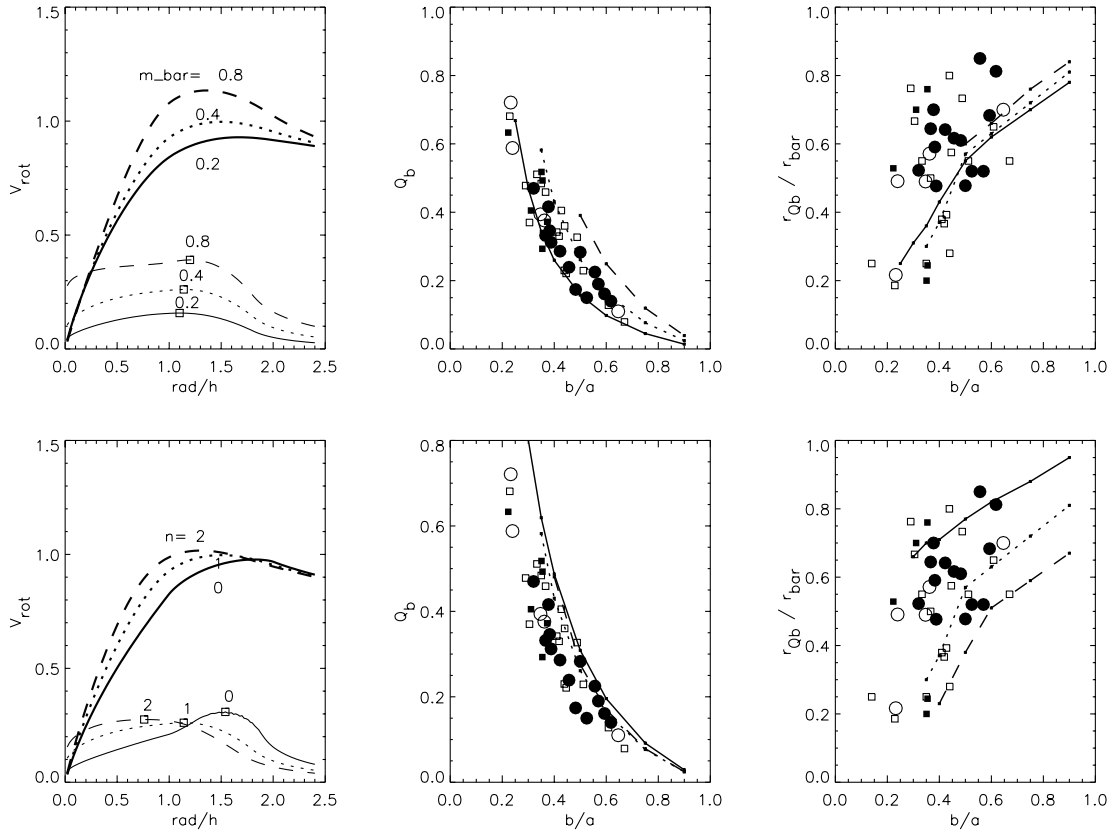


Figure 9. Same as Fig. 8, except that the bulge component is omitted, leading to more slowly rising central rotation curve.

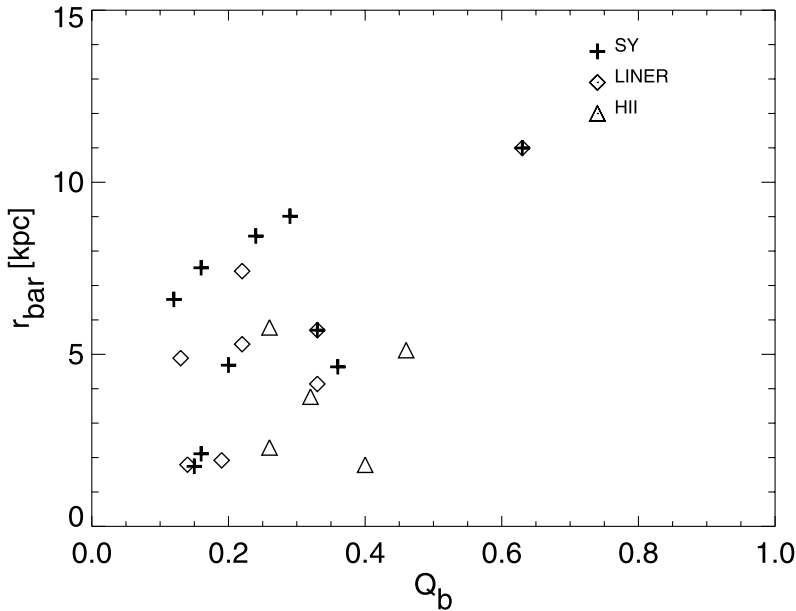


Figure 10. The absolute bar length r_{bar} versus bar strength Q_b for the active galaxies showing separately Seyfert 2 and Seyfert 1–1.5 galaxies, LINERs and H II galaxies. The mixed activity types are indicated by two superimposed symbols.

6 COMPARISON OF SEYFERTS, LINERS AND H II GALAXIES

We next compare the properties of bars in Seyferts, LINERs and H II galaxies. On the basis of the previous work by Martinet & Friedli (1997), H II galaxies typically reside in long bars, while bars in Seyferts might have on the average similar lengths as non-active

galaxies (Marquez et al. 2000). Shlosman et al. (2000) and Laine et al. (2001) found some evidence that Seyferts might miss bars with large ellipticities, but that has been contradicted by Marquez et al., who concentrated only on isolated galaxies.

We showed in Chapter 4 that bar length r_{bar} is weakly correlated with bar strength Q_b , but only for the late-type galaxies or for the non-active early-type spirals (see Fig. 7). A similar plot is shown

for Seyferts, LINERs and H II galaxies separately in Fig. 10. The interesting thing here is that the galaxies with the longest bars ($r_{\text{bar}} > 6$ kpc) are either type 1–1.5 Seyferts (3 galaxies) or intermediate types between LINERs and Seyferts 2 galaxies (1 galaxy), while for one of them the Seyfert type is not known. On the other hand, we have no identification of type 1–1.5 Seyferts among the Seyferts with shorter bars ($r_{\text{bar}} = 1.5 - 5$ kpc). One of them is identified as Seyfert 2, although for three of them the Seyfert type is not known. All the type 1–1.5 Seyferts here have early Hubble types, whereas the H II galaxies are mostly late-type systems.

Seyfert 2 galaxies generally have strong circumnuclear starbursts or may in some cases even have nuclear starbursts, so that in that sense they can be more closely associated with H II galaxies. Or at least the true active nuclei may be overshadowed by strong star-formation events. Also, as LINERs represent the lower-level nuclear activity, probably induced by a shock-heating mechanism, it is possible that the true active nuclei in terms of black holes and accretion discs are only the type 1–1.5 Seyferts. Therefore, if Sy1–1.5 galaxies could really be distinguished from LINERs, type 2 Seyferts and H II galaxies by their long but relatively weak bars that would probably be a new helpful piece of knowledge when discussing the formation and evolution of active galactic nuclei. However, our result is only of a preliminary nature and should be confirmed using a much larger sample of galaxies.

7 DISCUSSION

The connection between bars and nuclear activity has been a longstanding debate since the first efforts by Noguchi (1988) and Shlosman et al. (1989). They showed that non-axisymmetries in the background gravitational potential, e.g. stellar bars, intrinsic or induced by interactions, can cause redistribution of mass in galactic discs in such a way that it may help to ignite formation of an active nucleus. However, this connection has turned out to be extremely difficult to prove both theoretically and observationally.

On a quantitative scale, a large majority of spiral galaxies are barred. The situation becomes exceedingly interesting and complex, since minibars may be nested at the centres of larger bars (Regan & Mulchaey 1999; Martini & Pogge 1999; Eskridge & Frogel 1999). There is no indisputable agreement showing that Seyferts really have more bars than the non-active galaxies, and it is still a puzzle why nuclear activity appears in some barred galaxies, but does not exist in many of them. Of course, both for a nuclear starburst and for fuelling an active nucleus, a minimum amount of gas is needed. This condition seems to be well fulfilled in many barred galaxies, because they have on the average three times higher nuclear molecular gas surface densities than the unbarred galaxies (Sheth 2001). Therefore it is clear that enhanced gas density in the bar region is not a sufficient condition for the onset of nuclear activity.

The gas flow associated with the non-axisymmetric bar potential occurs both inward and outward, depending on the position with respect to the bar major axis. In the seminal papers by Athanassoula (1992a,b) it was shown that shock regions are accompanied by a strong inflow, so that net inflow becomes possible if high-density shocks are present. The form of shocks, and the strength of connected inflow depends crucially on the main orbital families of the potential: the eccentricity of the major axis, bar-supporting x_1 family, and the presence and extent of perpendicular x_2 orbits, associated with the ILR. Especially, off-axis shocks require the presence of x_2 orbits. The morphology of

the shock features in Athanassoula’s models explains well the observed shapes of dust lanes in barred galaxies, placing strict limits for the relation between the bar extent and its corotation radius for bulge-dominated galaxies. In general, more massive and more elongated bars lead to stronger inflow rate, due to larger density contrast between shock and non-shock regions. Later studies have confirmed the robustness of these results in terms of dependence on various numerical methods and model parameters (Patsis & Athanassoula 2000). However, the shock morphology and inflow is to some degree sensitive to the effective sound speed of gas, larger random motions favoring on-axis shocks and larger inflow (Englmaier & Gerhard 1997; Patsis & Athanassoula 2000).

The large fraction of active systems among our early-type barred galaxies (about 3/4) is in accordance with these shock models: the potential perturbation accompanied by $Q_b > 0.15$ or $\epsilon > 0.4$ is well in the range expected to cause a substantial inflow of gas. The fact that we find that a smaller fraction of active systems among the late-type barred spirals (1/4) is also as expected: reducing the central concentration of the galaxy potential (moving from early to late-type systems) first limits the extent of x_2 orbits and then makes them disappear altogether, which according to Athanassoula (1992b) replaces the strong off-axis shocks by the weaker on-axis shocks and finally makes the shocks disappear. In general, the active systems among our late-type barred galaxies all represent fairly large perturbation ($Q_b > 0.3$ or $\epsilon > 0.65$), although there are several non-active galaxies with similar perturbation strengths.

Indeed, some important questions arise from our measurements. For example, why is the average bar strength smaller for the active than for the non-active galaxies of a similar morphological type (early-type galaxies)? Also, why is there no correlation between bar strength and length for the active early-type galaxies? Most surprising is our finding that the average perturbation in the non-active early-type galaxies is much higher than that for the active early-type galaxies. Especially, our sample contains four non-active early-type galaxies with $Q_b > 0.4$ ($\epsilon > 0.63$), for which high inflow rate would be expected (see Fig. 4). Perhaps these systems represent a case where the previous inflow has been so efficient that the fuel available for an active nucleus has already been consumed. Or perhaps too strong bars in general are not favourable for supporting nuclear activity: only two of our active galaxies have a perturbation in the above range, but for them r_{Q_b}/h is very large.

In general, the moderately weak bar potential favours the inflow of gas toward a nuclear ring connected to ILR, provided that the bar pattern speed is not so high that ILR is completely absent. A nuclear ring represents in itself a rather stable configuration, which, however, might become susceptible to further dynamical instabilities via gradual build-up of material, as in the original minibar scenario by Shlosman et al. (1989): these additional mechanisms would then be responsible for the actual AGN activity. On the other hand, according to the models by Athanassoula (1992b) very strong bars (massive or highly elongated) lead to the disappearance of x_2 orbits. Consequently, instead of accumulating to nuclear rings the gas flows directly toward centre, which perhaps is not an ideal condition for the further feeding mechanisms to operate. The fact that the active early-type galaxies were found to have force maxima at rather large distances also supports the presence of x_2 -orbits: these bars probably have fairly flat density profiles, resembling the homogeneous bar models in Athanassoula (1992b) with substantial extent of x_2 orbits. Also, their bars were found to be fairly long, suggesting slow rotation and thus the presence of ILR.

The formation and evolution of bars is a complicated process, in which secular evolution both in terms of isolated evolution and galaxy interactions might play an important role, thus changing the barred properties or even the Hubble type. In general, for weak bars to develop, the dynamical instabilities must be rather small in the inner regions of the discs. This kind of condition can be produced in simulations for example by increasing the stellar velocity dispersion so that the Toomre parameter is $2 < Q < 3$ (Athanasoulas 1992a; Rautiainen & Salo 2000), by cold and lumpy gas in the disc (Shlosman & Noguchi 1993) or by central mass concentrations like compact bulges, nuclear star clusters or supermassive black holes (Hasan & Norman 1990; Hasan, Pfenniger & Norman 1993; Norman, Sellwood & Hasan 1996). This kind of compact structure leads to a subsequent weakening of the bar and finally even to its dissolution.

Compact bulges can be formed for example in the evolution processes of bars, where thickening of the inner particle distribution occurs when the bar dissolves, as discussed by Norman et al. (1996). This dense mass concentration gradually reduces the volume of phase space accessible to regular, bar-supporting orbits of the x_1 family. In some of their models the bar was only weakened during the formation of the new bulge, but in some cases it was completely destroyed. This kind of secular evolution gives one possible explanation why bars can be either strong or weak among galaxies with large bulges (active and non-active early-type galaxies), but in this scenario it is less clear why the activity should appear especially in the more weakly barred galaxies, e.g. in those where the bulges are suggested to be relics of earlier bars. Especially, what mechanism would in that case feed the nucleus? Alternatively, the non-active early-type galaxies (with large bulges) might also be candidates for the relics of this kind of secular evolution of bars. What we could do is for example to look at the morphological types of bars in more detail. For example, in the models by Norman et al. (1996) the newly-formed bulges never have boxy shapes. Also worth looking at are the two different bar components that sometimes appear simultaneously in galaxies, the thick bar component composed of a warm stellar population, and the thin spindle made of a cool population (Block et al. 2001). These two bar components are possibly formed at different epochs in the life of the galaxy and therefore might be indicators of secular evolution.

There is some evidence that galaxy interactions may also play an important role in the formation of bars (Noguchi 1988, 1996; Salo 1991). In the models by Noguchi (1996) strong bars can develop after the pericentre passage, the bars formed being long-lasting with little change in their strengths or lengths. The intensity profiles of bars produced in tidal processes are typically flat, while those produced without any external triggering are more rapidly declining. This fits to the observations of Elmegreen & Elmegreen (1985), who showed that bars in early-type galaxies are often flat, whereas in the Hubble types of Sc or later bars are generally exponential. According to Noguchi the weak response in the galactic disc to the bar instability is ascribed to highly dissipative gas, which effectively stabilizes the stellar discs by creating large stellar clumps leading to effective heating of the disc (Shlosman & Noguchi 1993). In this scenario the exponential bars, contrary to the flat bars, are not created from the disc being rather bulge components deformed by the bar instability (Noguchi 2000).

The environmental study of normal galaxies by Elmegreen, Bellin & Elmegreen (1990) gives some support to the interaction scenario. They showed that among the early Hubble types the fraction of barred galaxies is twice as high in binaries as in field

galaxies or galaxies in groups, suggesting a strong link between close interactions and flat bars. Therefore one would expect that Seyfert galaxies, which appear preferentially in early-type spirals, would also frequently have bars and appear in crowded galaxy environments. Indeed, Seyferts may have more bars than the non-active galaxies, but contrary opinions also appear. However, it is promising that the frequency of Seyfert activity is clearly increased only in the barred early-type galaxies (Laurikainen & Salo, in preparation), which indicates that after all, large-scale bars might somehow be controlling the nuclear activity. Concerning the galaxy environments there are at least two observational results showing that galaxy interactions should not be forgotten while discussing Seyfert activity. Namely, Seyferts avoid strongly disrupted interacting systems (Keel et al. 1985; Bushouse 1987), which is in the same line with our result showing that active galaxies generally have rather small non-axisymmetric forces in the inner discs. And secondly, Seyfert 2 galaxies seem to appear more frequently in interacting systems (Laurikainen & Salo 1995; de Robertis, Yee & Hayhoe 1998; Dultzin-Hacyan et al. 1999) and have on the average more companions than the type 1 Seyferts or the non-active galaxies (Laurikainen & Salo 1995).

In order to disentangle the full dynamical stages of bars in the galaxies studied here it would be important to compare the length and strength properties with the high-resolution gas-kinematical observations available for nearby galaxies. This would, for example, highlight the connection between bar strength and gas inflow and possibly also give some perspective on the evolutionary scenarios of bars. It would also be important to understand in more detail how and to what extent the bulges may control the barred properties and consequently the nuclear activity in galaxies.

8 CONCLUSIONS

We have compared bar strengths in active and non-active galaxies for a sample of 43 barred galaxies. In order to consider only the clear cases, identification of a bar was done in the near-IR by Fourier techniques from an original sample of 107 disc galaxies. Bar strengths were estimated by a new method (Buta & Block 2001) of calculating the tangential forces, normalized to the axisymmetric radial force field $Q_T(R) = [F_T(R)]_{\max}/\langle F_R(R) \rangle$. In order to have a single measure for the bar strength, the maximum tangential force, Q_b , in the bar region was used. We also verified how well the ellipticity of a bar correlates with Q_b .

In the analysis we used *JHK*-images of the 2 Micron All Sky Survey (2MASS) by constructing mosaics for most of the galaxies. Some analytical force models were also applied to the interpretation of our observational results, in which model bars were described by Ferrers ellipsoids. One of the most important results in this work is that favourable conditions for the onset of nuclear activity seem to be met in those early-type galaxies where the non-axisymmetric forces are rather small in the inner discs.

The main conclusions are the following.

- (i) *The maximum ellipticity ϵ of the bar correlates quite well with the maximum tangential force Q_b in the bar region.* This is a first clear empirical indication showing that ϵ can be used as a measure of the bar strength. Based on our toy models, the small scatter in the diagram can be understood by means of different bar mass fractions in galaxies. Alternatively, the dispersion can be partly due to the uncertainties in the vertical scaleheights of the galactic discs.
- (ii) *The distance of the peak ellipticity, r_ϵ in the bar region, generally used as a measure of the bar length, systematically*

underestimates the length of the bar. This was verified by comparing r_ϵ with r_{bar} , obtained by Fourier analysis.

(iii) *In the active early-type galaxies, bars are on the average weaker (and their maximum ellipticities are smaller) than in their non-active counterparts or in the late-type galaxies.* The KS-test shows that the probability that the samples of active and non-active early-type galaxies are drawn from similar populations is $p = 0.04$ and 0.02 for Q_b and ϵ , respectively, the differences thus being statistically significant. The mean Q_b values for the samples of active and non-active early-type galaxies are 0.21 ± 0.07 and 0.35 ± 0.19 .

(iv) On the other hand, the scaled distances of the maximal tangential forces or ellipticities, r_{Q_b}/h and r_ϵ/h in the bar region, are largest for the active early-type galaxies. The differences in r_{Q_b}/h and r_ϵ/h between the active and non-active early-type galaxies are statistically significant with $p = 0.0008$ and $p = 0.007$. The mean r_{Q_b}/h for the two subsamples of early-type galaxies are 1.24 ± 0.58 and 0.51 ± 0.28 , respectively. In comparison with active early-type galaxies the values of these parameters are somewhat smaller for the active late-type systems, and smallest for the non-active galaxies of any Hubble type.

(v) We confirm the earlier result by Elmegreen & Elmegreen (1985), Martin (1995) and Regan & Elmegreen (1997) showing that bars are on the average longer for the early- than for the late-type galaxies. However, the dispersion especially for the early-type galaxies is very large.

(vi) *Bar length r_{bar} does not correlate with bar strength Q_b for the active early-type galaxies;* rather, short bars can have either weak, moderate or strong non-axisymmetric forces. However, a weak correlation appears for the active late-type galaxies and for all the non-active galaxies showing an increasing bar strength with the increasing bar length.

ACKNOWLEDGMENTS

This publication makes use of data products from the 2 Micron All Sky Survey, which is a joint project of the University of Massachusetts and the Infrared Processing and Analysis Center/California Institute of Technology, funded by the National Aeronautics and Space Administration and the National Science Foundation. It also uses the NASA/IPAC Extragalactic Database (NED), operated by the Jet Propulsion Laboratory in Caltech. We acknowledge the foundations of Magnus Ehrnrooth, Väisälä and Wihuri and the Academy of Finland for significant financial support.

REFERENCES

Aquerri J. A. L., 1999, *A&A*, 351, 43
 Athanassoula E., 1983, *A&A*, 127, 349
 Athanassoula E., 1992a, *MNRAS*, 259, 328
 Athanassoula E., 1992b, *MNRAS*, 259, 345
 Baggett W. E., Baggett M., Anderson K. S. J., 1998, *AJ*, 116, 1626
 Bushouse H. A., 1987, *ApJ*, 320, 49
 Buta R., Block D. L., 2001, *ApJ*, 550, 243
 Block D. L., Wainscoat R. J., 1991, *Nat*, 353, 48
 Block D. L., Puerari I., Knapen J. H., Elmegreen B. G., Buta R., Stedman S., Elmegreen D. M., 2001, *A&A*, 375, 761
 Combes F., Sanders R. H., 1981, *A&A*, 96, 164
 de Grijs R., 1998, *MNRAS*, 299, 595

de Jong R. S., 1996, *A&A*, 313, 45
 de Robertis M. M., Yee H. K. C., Hayhoe K., 1998, *ApJ*, 496, 93
 de Vaucouleurs G., de Vaucouleurs A., Corwin H. G., Jr, Buta R., Paturel G., Fouque P., 1991, *Third Reference Catalogue of Bright Galaxies*. Springer-Verlag, New York (RC3)
 Dultzin-Hacyan D., Krongold Y., Fuentes-Guridi I., Marziani P., 1999, *ApJ*, 513, L111
 Duval M. F., Monnet G., 1985, *A&AS*, 61, 141
 Elmegreen B. G., Elmegreen D. M., 1985, *ApJ*, 288, 438
 Elmegreen B. G., Bellin A., Elmegreen D., 1990, *ApJ*, 364, 415
 Englmaier P., Gerhard O., 1997, *MNRAS*, 287, 57
 Eskridge P. B., Frogel J. A., 1999, *Ap&SS*, 269, 427
 Hasan H., Norman C., 1990, *ApJ*, 361, 69
 Hasan H., Pfnegner D., Norman C., 1993, *ApJ*, 409, 91
 Ho L. C., Filippenko A. V., Sargent W. L. W., 1997, *ApJ*, 487, 591
 Hunt L. K., Malkan M. A., 1999, *ApJ*, 516, 660
 Keel W. C., Kennicutt R. C., Jr, Hummel E., van der Hulst J. M., 1985, *AJ*, 90, 708
 Knapen J. H., Shlosman I., Peletier R. F., 2000, *ApJ*, 529, 93
 Kormendy J., 1979, *ApJ*, 227, 714
 Laine S., Shlosman I., Knapen J. H., Peletier R. F., 2001, preprint (astro-ph/0108029)
 Laurikainen E., Salo H., 1995, *A&A*, 293, 683
 Laurikainen E., Salo H., 2000, *A&AS*, 141, 103
 Laurikainen E., Salo H., 2002, *MNRAS*, submitted
 Laurikainen E., Salo H., Rautiainen P., 2001, in Knapen J. H., Beckman J. E., Shlosman I., Mahoney T. J., eds, *ASP Conf. Ser. Vol. 249, The Central kpc Starburst and AGN*. Astron. Soc. Pac., San Francisco
 Malkan M. A., Gorjian V., Tam R., 1998, *ApJS*, 117, 25
 Marquez I. et al., 2000, *A&A*, 360, 431
 Martin P. R., 1995, *AJ*, 109, 2428
 Martinet L., Friedli D., 1997, *A&A*, 323, 363
 Martini P., Pogge R. W., 1999, *AJ*, 118, 2646
 McLeod K. K., Rieke G. H., 1995, *ApJ*, 441, 96
 Moles M., Marquez I., Perez E., 1995, *ApJ*, 438, 604
 Mulchaey J. S., Regan M. W., 1997, *ApJ*, 482, L135
 Noguchi M., 1988, *A&A*, 203, 259
 Noguchi M., 1996, *ApJ*, 469, 605
 Noguchi M., 2000, *MNRAS*, 312, 194
 Norman C. A., Sellwood J. A., Hasan H., 1996, *ApJ*, 462, 114
 Ohta K., 1996, in Buta R., Crocker D., Elmegreen B., eds, *IAU Colloquium 157, Barred Galaxies*. ASP, San Francisco, p. 37
 Patsis P., Athanassoula E., 2000, *A&A*, 358, 45
 Pfnegner D., 1984, *A&A*, 134, 373
 Quillen A. C., Frogel J. A., Gonzalez R. A., 1994, *ApJ*, 437, 162
 Rautiainen P., Salo H., 1999, *A&A*, 348, 737
 Rautiainen P., Salo H., 2000, *A&A*, 362, 465
 Regan M. W., Elmegreen D. M., 1997, *AJ*, 114, 965
 Regan M. W., Mulchaey J. S., 1999, *AJ*, 117, 2676
 Salo H., 1991, *A&A*, 243, 118
 Salo H., Rautiainen P., Buta R., Purcell G. B., Cobb M. L., Crocker D. A., Laurikainen E., 1999, *AJ*, 117, 792
 Sakamoto K., Baker A. J., Scoville N., 2000, *ApJ*, 533, 149
 Sheth K., 2001, in Knapen J. H., Beckman J. E., Shlosman I., Mahoney T. J., eds, *ASP Conf. Ser. Vol. 249, The Central kps Starburst and AGN*. Astron. Soc. Pac., San Francisco
 Shlosman I., Noguchi M., 1993, *ApJ*, 414, 474
 Shlosman I., Frank J., Begelman M., 1989, *Nat*, 338, 45
 Shlosman I., Peletier R. F., Knapen J. H., 2000, *ApJ*, 535, L83
 Tully R. B., 1988, *Nearby Galaxies Catalogue*. Cambridge Univ. Press, Cambridge

This paper has been typeset from a $\text{\TeX}/\text{\LaTeX}$ file prepared by the author.